American Journal of Condensed Matter Physics 2024, 13(3): 45-50
DOI: 10.5923/j.ajcmp.20241303.01

Ab Initio Study of Hydrogen Adsorption on Lanthanum Chromium Oxide ($LaCrO_3$) (001) Surface as Potential Solid Oxide Fuel Cell Material

Oyedare Peter Olusola[1], Jibril Ibrahim Manya[2], Maharaz M. Nasir[3], Alhassan Shuaibu[2,*]

[1]Science Laboratory Department Federal Polytechnic Ede, Osun State, Nigeria
[2]Department of Physics, Kaduna State University, Kaduna, Kaduna, Nigeria
[3]Department of Physics Federal University Dutse, Jigawa State

Abstract Density functional theory plus Hubbard (DFT+U) calculations were employed to investigate the adsorption of Hydrogen (H)-adatom on the (001) surface of $LaCrO_3$ (LCrO). The adsorption is found to be stable with H binding preferentially at Cr site on the LaO-terminated surface. The adsorption of H molecule also leads to the electrons transferring from the substrate to the charges rearrangement within the compound. We further predict the adsorption energies of Hydrogen adsorption sites on LCrO (001) surface. Based on the adsorption energy comparison, LCrO is more hydrogenation-tolerant than traditional Ni-based anode materials, which is qualitatively in line with available experimental results. This study provides a scientific basis for rational design of Hydrogen-tolerant intermediate temperature materials for Solid oxide fuel cell (SOFCs).

Keywords Density functional theory plus Hubbard (DFT+U), $LaCrO_3$ (LCrO), Hydrogen adsorption and Solid oxide fuel cell (SOFC)

1. Introduction

Solid oxide fuel cell (SOFC) provides a new and clean electric power generation system [1]. At present, Y_2O_3 stabilized ZrO_2 (YSZ) is commonly used for the electrolyte of solid oxide fuel cell [2]. Since the oxide ion conductivity of YSZ is insufficient for the electrolyte of fuel cells, a thin electrolyte film without gas leakage and an excessively high operating temperature such as 1273 K, are essential for the high power density of SOFCs when YSZ is used as the electrolyte [3]. On the other hand, all advantages of SOFC such as a high efficiency and a variety of usable fuel can be obtained at decreased temperatures such as 1073 K. Furthermore, the choice of materials for the cell stacking becomes wide; in particular, cheap refractory metals such as stainless steel will be usable by decreasing the operating temperature down to 1100 K [4]. Consequently, the decrease in the operating temperature becomes the critically important subject for the development of cheap but reliable cells [5].

Decreasing the operating temperature requires an active electrode, in particular, a cathode catalyst and an electrolyte with a low resistance. Ceria doped with Gd or Sm is generally considered for the electrolyte of SOFC operable in the decreased temperature range [6]. However, ceria based oxide exhibits n-type semi conduction in the reducing atmosphere [7]. Consequently, n-type semi conduction drastically decreases the open circuit potential compared to the theoretical values [8]. In addition, some amount of fuel is consumed by oxygen leakage W to the internal short circuited state of the electrolytes by formed electrons. It is also reported that the expansion due to the reduction causes a severe stress on electrolytes which sometimes become higher than the intrinsic mechanical strength of CeO_2 fuel cell oxide [9]. Therefore, there are some problems which should be solved for CeO based oxide cells. On the other hand, preparing very thin YSZ film is also investigated for intermediate temperature SOFC [10], however, the reliability becomes low when the thickness of the electrolyte becomes extremely thin and furthermore, it is anticipated that the power density may become unstable by using very thin YSZ film for electrolyte.

It is, therefore, of great importance to develop new electrolyte materials which exhibit high oxide ion conduction over a wide oxygen partial pressure range. The reports on the oxide ion conductivity are limited on oxides with non-fluorite structure. In a recent study, it was observed that oxide ion conductivity in the oxide with perovskite structure was investigated within both theory and experiment was found that the $LaCrO_3$-based perovskite type oxide exhibits

* Corresponding author:
alhassa.shuaibu@kasu.edu.ng (Alhassan Shuaibu)
Received: Dec. 2, 2024; Accepted: Dec. 23, 2024; Published: Dec. 28, 2024
Published online at http://journal.sapub.org/ajcmp

high oxide ion conductivity [11], which is comparable with that of CeOz- based oxide. In particular, $LaCrO_3$ doped with Sr for La and Mg for Cr sites exhibits high oxide ion conductivity stable over a wide oxygen partial pressure range, the high oxide ion conductivity of this oxide system was reported by several other researchers. The advantage of this oxide is that almost pure oxide ion conductivity is exhibited in both reducing and oxidizing atmospheres. It is reported that the electron and hole conduction is smaller than that of oxide ion by a few orders of magnitude. It is, therefore, expected that the operating temperature of SOFC can be decreased by using $LaCrO_3$-based oxide for the electrolyte of SOFCs.

But a major drawback of $LaCrO_3$-based perovskite when to be consider as a solid oxide fuel cell (SOFC) material is that it can experience structural and performance instability. Another issue to be considering is that the cathode the site of the oxygen reduction reaction becomes the limiting component in a SOFC as temperatures are lowered, when $LaCrO_3$ is to be used. Hence, by surface modification, or doping such drawback can be address. The Hydrogen (H) absorption on surface of other perovskite material has shown such ability, therefore, this work used computational method to study the hydrogen Absorption on $LaCrO_3$ surface within the frame of Density functional theory plus Hubbard (DFT+U) As Potential Material for Applications in Intermediate Temperature Solid Oxide Fuel Cells.

2. Computational Details

First-principles DFT+U total energy calculation are carried out as implemented in the Quantum ESPRESSO code [12], in which the plane-wave pseudopotential total energy calculation method based on the DFT is used. The interaction between nuclei and electrons is approximated with Vanderbilt ultrasoft pseudopotential [13] and the Perdew-Wang-91 parametrization [14] is taken as the exchange-correlation functional in the generalized- gradient approximation. After test calculation, kinetic energy cutoff at 420 eV and the Brillouin zone sampling 12×12×1 and 8×8×1 Monkhorst–Pack [15] *k*-points for surface is adopted. By further increasing the kinetic energy cutoff and the number of *k*-points the change in the results could be neglected. La, Cr, O, S, H atoms are described by La($5s^2 5p^6 5d^1 6s^2$), Cr($3d^5 4s^1$), O($2s^2 2p^4$), S($3s^2 3p^4$), H($1s^1$) valence electrons, respectively. A relaxation is performed for the constructed supercell by using Broyden–Fletcher–Goldfarb–Shanno algorithm [16] to minimize the energy with respect to atomic position. In calculations the tolerances for self-consistence are set at 1.0×10^{-6} eV $atom^{-1}$ for total energy, 0.05 eV $Å^{-1}$ for force, 2.0×10^{-5} eV $atom^{-1}$ for band energy, 0.1 GPa for maximum stress and 0.002 Å for the maximum displacement.

In this study, we consider orthorhombic perovskite structure of orthorhombic structure with space group *Pbnm* since the structural phase transition to orthorhombic symmetry was suggested to occur above high temperature [17]. The Jahn–Teller distortion may not be critical under SOFCs operating conditions.

We model the adsorbate adsorption on a much less polar $LCrO_3$ (001) surface with respect to $LCrO_3$ (110) surface consisting of alternating CrO_2/LaO plane. The structure with GGA+U parameters is shown in Figure 1.

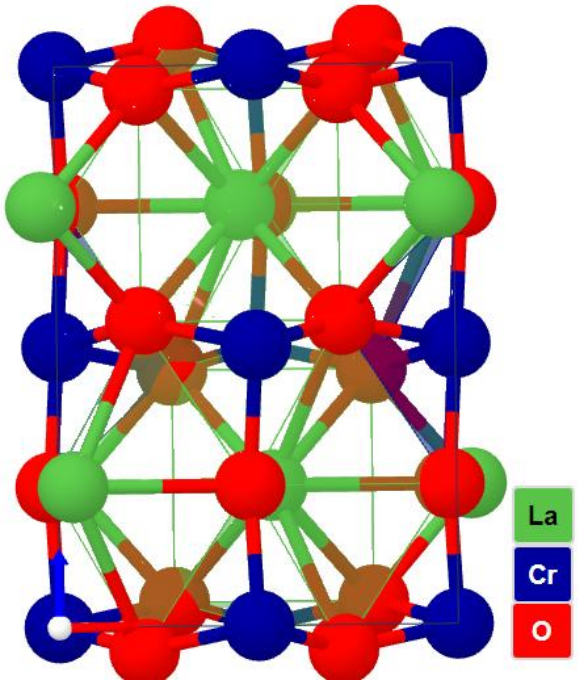

Figure 1. Structure of Pure $LaCrO_3$ with GGA+U optimized parameters

Table 1. Calculated lattice parameters a,b,c, the related experimental data and other theoretical works for $LaCrO_3$

S/n	Materials	*a* (Å)	*b* (Å)	*c* (Å)	Reference
1	**$LaCrO_3$**	**5.561**	**7.879**	**5.608**	**This Work**
2	$LaCrO_3$	5.500	7.800	5.500	Theory [a]
3	$LaCrO_3$	5.500	5.500	5.500	Theory [a]
4	$LaCrO_3$	5.520	5.500	7.780	Theory [b]
5	$LaCrO_3$	5.508	7.791	5.484	Theory [c]
6	$LaCrO_3$	5.479	5.516	7.766	Theory [d]
7	$LaCrO_3$	5.479	7.756	5.516	Experimental [e]
8	$LaCrO_3$	5.439	7.691	5.458	Experimental [f]
9	$LaCrO_3$	5.444	5.444	13.094	Experimental [g]
10	$LaCrO_3$	5.508	7.791	5.484	Experimental [g]

Table 2. Bond lengths (Å) between two nearest neighbouring atoms of pure $LaCrO_3$

S/N	Nabouring Atoms	Bond Length Pure $LaCrO_3$ (Å)
1	L-Cr	2.6134
2	L-O	2.6611
3	Cr-O	2.2582
4	Cr-Cr	5.6066
5	L-L	4.8866

Furthermore the bonds length between the two neighboring atoms of the pure $LaCrO_3$ were measured which

is the equilibrium distance between the nuclei of two groups or atoms that are bonded to each other, bond lengths is a property of a chemical bond between types of atoms. It has been reported in Table 2, our results show with many reported results with approximate error between 1% to 2%.

Electronic Properties of Pure Lanthanum Chromium Oxide

Calculated Density of State (DOS) for Pure $LaCrO_3$

Here, we focus on analyzing the atomic partial density of states (PDOS) of bulk $LCrO_3$ as shown in Figure 2.

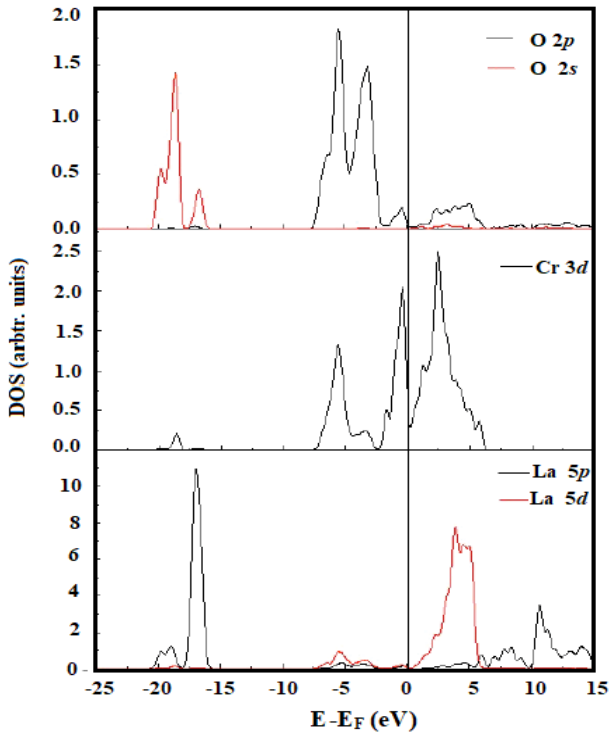

Figure 2. Calculated PDOS for pure orthorhombic $LaCrO_3$ with GGA+ U optimized parameters. The zero point of the energy axis corresponds to the Fermi level

From the graph it observed that the orbital hybridization between Cr 3d and O 2p, O 2s and La 5p states is found, which dominates the main electronic properties of $LCrO_3$. The top of valance bands consists of Cr 3d and O 2p and the bottom of conduction bands are mainly composed of the La 5d and Cr 3d states. Further, our calculated results (see Table 1) show good agreement with the theoretical and photoemission data [21]. As an example, experimental studies show that the La 5p orbitals are located around –20.8 eV, and our calculations show that they are around –22.0 eV.

Table 3. Comparison of the orbital energy level (energy values correspond to the peaks in the DOS curve)

	$LaCrO_3$		
	La 5p	O 2s	O 2p (eV)
Experimental	–18.0	–22.5	–6.5
Calculation	–20.1	–22.7	–5.9
This work	–22.0	–20.8	–8.6

Calculated Band Structure for Pure $LaCrO_3$

The band structure of a material is an important characteristic of its electronic structure. The path in *k*-space along which the bands have been computed is defined as $\Gamma - X - S - Y - \Gamma - Z - U - R - T$ in order to correspond to what is found in literature for orthorhombic cells [18].

Figure 3 shows our calculated band structure of LaCrO3 with GGA+U (U=3.12), Here, it is observed that $LaCrO_3$ has a direct band gap at the Γ with gap value of about 2.65 eV which is really in agreement with many theoretical reports [19] and also closed to the experimental value [20]. In addition to direct band gap nature of our result, the balanced charge transportation i.e. the electron and hole have similar effective mass looking at the conduction band CB and valance band VB nature of the graph, this character is superior nature to the lead perovskite $CH_3NH_3PbI_3$ when use in solid state fuel cell [20]. In conventional semiconductors such as GaAs and $CuInSe_2$, the hole effective mass (mainly contributed from localized anion p orbital) is higher than electron effective mass (mainly contributed from delocalized cation s orbital). The hole effective mass in oxides is even higher due to strong electronegativity of oxygen atom, this strong electronegativity nature indicate a strong property of using $LaCrO_3$ as potential material for intermediate temperature material in solid state fuel cell.

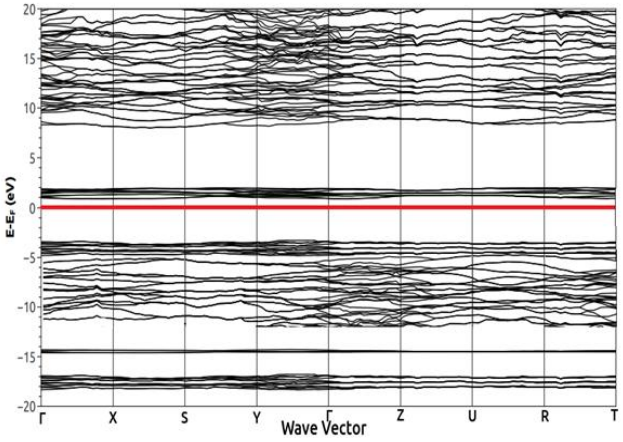

Figure 3. Calculated Band Structure for Pure $LaCrO_3$ with our optimized GGA+U (U=3.12 eV) parameters (the red line at 0 indicate the Fermi level)

The effect of Hydrogen adsorption at perfect $LaCrO_3$ (001) surface

The hydrogen adsorption process is critical to the properties of SOFC anode. The adsorption of H at the clean LCO (001) surface has been investigated using the DFT+U optimized parameters. The adsorption energy is calculated with the formula in Ref. [24] An optimized crystal structure of H adatom terminated at the LCO (001) surface is shown in Figure 4.

The computed H adsorption properties are also presented in Table 4. We can conclude that adatom H occupies the Cr site and La site with the adsorption energies of 3.157 and 3.097 eV, respectively. The Cr and La sites are more stable than two O sites; there is a consistent preference for SH

adsorption results over the two terminated surface of $LaCrO_3$ reported by [25]. Among four positions, the Cr site is the most energetically favorable. Along with comparison of our obtained results for the reported results in [26] for similar material LaFeO3, it should be predicted that the adsorption energies of the H-containing species in all the configurations on two terminated surface increase. This is consistent with the H-containing species adsorbed on MgO (100) surface [22] and Cu, Ni, Ag, Pd (111) surfaces [23].

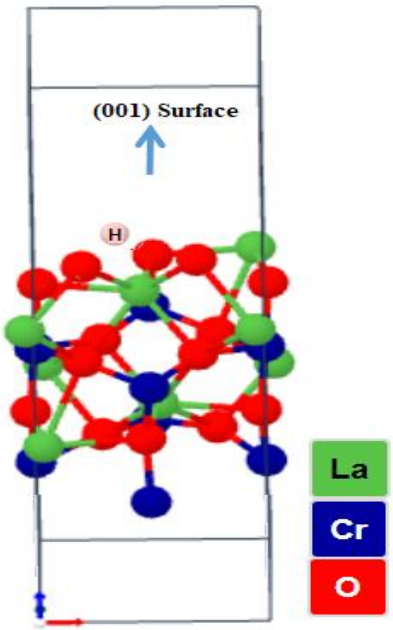

Figure 4. Schematic representation of the optimized $LCrO_3$ (001) surface with Hydrogen terminated adatom

Table 4. Calculated adsorption properties for H atom on $LCrO_3$ (001) surface

Ads. site	E_{ads} (eV)	Distance (Å)	Bond population (e)	Charges (e)
		$H–M_{Hydrogen}$	$H-M_{Hydrogen}$	H
CrO_2(001)				
O-1	2.795	1.691	0.27	0.13
Cr	3.157	2.034	0.85	–0.05
LaO-(001)				
O-2	2.663	1.762	0.09	–0.19
La	3.097	2.671	0.76	–0.39

The calculated $H–M_{Hydrogen}$ distance in four adsorption sites varies from 1.691 to 2.671 Å . All the bond populations of $H–M_{Hydrogen}$ are positive, which demonstrates that covalent bonds between H atoms and substrate atoms are formed. The calculated effective charges indicate that charges transfer after H adsorption. With the exception of O-1 site, the charges of H are negative and H behaved as electron acceptors. The density of states (DOS) analysis also can provide fundamental understanding of the adsorbate substrate interaction. The atomic PDOS are depicted in Figure 5 for adatom H at the most favored Cr site and the nearest neighbor Cr atom on the surface. Adsorbate H 1s states are located from –10.7 to –12.6 eV with respect to the Fermi level, while in other energy regions the total DOS are predominantly contributed by H 1p states.

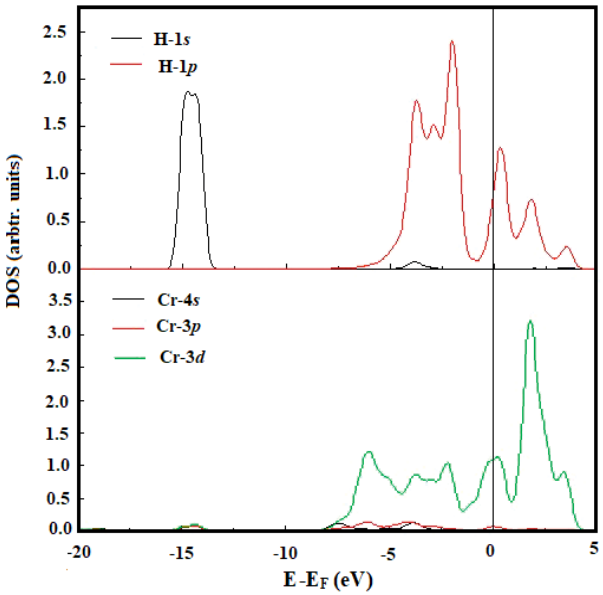

Figure 5. The PDOS for adatom H in Cr sites and the nearest neighbor Cr atom on the surface. The Fermi level is set to zero on the energy scale

For the nearest substrate Cr atom from H, the total DOS are largely dominated by Cr 3d states in the energy range from –6.36 to 3.40 eV. It can be seen that the hybridization between the Cr 3d states and H 1p states is quite strong around the energy level –3.65 to 3.09 eV. Moreover, one slight peak is observed between H 1s orbitals and Cr 4d, 3s, 3p orbital at about –11.6 eV.

Furthermore, the lower adsorption energies of 2.663–3.157 eV for H atom on LCrO surface compared to those on metal surfaces the H adsorption on Ni(111) surface have adsorption energies of 3.74–5.48 eV. The results of the adsorption properties indicate that the adsorption of H atom is slightly enhanced the conductivity and others properties of $LaCrO_3$ and H adatom favorably dissociated. These calculated results indicate that the H-absorption may be a good way to improve the structural stability and electrochemical property of LCO and can be used in anode of S as intermediate temperature [27].

3. Conclusions

Hydrogen tolerance on the perovskite-type materials LCrO3 is investigated by means of DFT+U calculations. Our calculated PDOS of bulk LCrO3 shows good agreement with the photoemission data and theoretically calculated values. Hydrogen adsorption is found to be stable with binding preferentially at Cr site on the LaO-terminated surface. The adsorption of Hydrogen adatom leads to the electrons transferring from the substrate to the adatom and the charges rearrangement within the molecule. In addition, the adsorption results of the corresponding H-containing dissociated species are obtained.

Both the species are found to be preferentially adsorbed at the Cr site. Both bond population and PDOS analysis show that there is hybridization between adatom H adatom and surface Cr atoms. Based on the adsorption energy comparison, LCrO is more Hydrogen-tolerant than traditional Ni-based anode materials used in SOFC, which is qualitatively in line with available experimental results. This study provides a meaningful basis for hydrogen-tolerant anode development as intermediate temperature in SOFC.

ACKNOWLEDGEMENTS

We thank and acknowledged the Department of Physics, Kaduna State University for providing the computing facilities used in this work.

REFERENCES

[1] Ni, M., Leung, M. K., & Leung, D. Y. (2008). Technological development of hydrogen production by solid oxide electrolyzer cell (SOEC). International journal of hydrogen energy, 33(9), 2337-2354.

[2] Gödickemeier, M., Sasaki, K., Gauckler, L. J., & Riess, I. (1997). Electrochemical characteristics of cathodes in solid oxide fuel cells based on ceria electrolytes. Journal of the Electrochemical Society, 144(5), 1635.

[3] Tuller, H. L., & Nowick, A. S. (1975). Doped ceria as a solid oxide electrolyte. Journal of the Electrochemical Society, 122(2), 255.

[4] Khorshidi, N. (2010). In-situ X-ray studies of model electrode surfaces for solid oxide fuel cells.

[5] Ishihara, T. (2009). Oxide ion conductivity in perovskite oxide for SOFC electrolyte. In Perovskite oxide for solid oxide fuel cells (pp. 65-93). Springer, Boston, MA.

[6] Sunarso, J., Hashim, S. S., Zhu, N., & Zhou, W. (2017). Perovskite oxides applications in high temperature oxygen separation, solid oxide fuel cell and membrane reactor: a review. Progress in Energy and Combustion Science, 61, 57-77.

[7] Lei, L., Zhang, J., Yuan, Z., Liu, J., Ni, M., & Chen, F. (2019). Progress report on proton conducting solid oxide electrolysis cells. Advanced Functional Materials, 29(37), 1903805.

[8] Sakai, N., Yokokawa, H., Horita, T., & Yamaji, K. (2004). Lanthanum chromite-based interconnects as key materials for SOFC stack development. International Journal of Applied Ceramic Technology, 1(1), 23-30.

[9] Solangi, K. H., Islam, M. R., Saidur, R., Rahim, N. A., & Fayaz, H. (2011). A review on global solar energy policy. Renewable and sustainable energy reviews, 15(4), 2149-2163.

[10] Wachsman, E. D., Marlowe, C. A., & Lee, K. T. (2012). Role of solid oxide fuel cells in a balanced energy strategy. Energy & Environmental Science, 5(2), 5498-5509.

[11] Brett, D. J., Atkinson, A., Brandon, N. P., & Skinner, S. J. (2008). Intermediate temperature solid oxide fuel cells. Chemical Society Reviews, 37(8), 1568-1578.

[12] Giannozzi, P., Andreussi, O., Brumme, T., Bunau, O., Nardelli, M. B., Calandra, M., ... & Baroni, S. (2017). Advanced capabilities for materials modelling with Quantum ESPRESSO. Journal of physics: Condensed matter, 29(46), 465901.

[13] Garrity, K. F., Bennett, J. W., Rabe, K. M., & Vanderbilt, D. (2014). Pseudopotentials for high-throughput DFT calculations. Computational Materials Science, 81, 446-452.

[14] Hamann, D. R. (2013). Optimized norm-conserving Vanderbilt pseudopotentials. Physical Review B, 88(8), 085117.

[15] Burke, K., Perdew, J. P., & Wang, Y. (1998). Derivation of a generalized gradient approximation: The PW91 density functional. In Electronic density functional theory (pp. 81-111). Springer, Boston, MA.

[16] Choudhary, K., & Tavazza, F. (2019). Convergence and machine learning predictions of Monkhorst-Pack k-points and plane-wave cut-off in high-throughput DFT calculations. Computational materials science, 161, 300-308.

[17] Head, J. D., & Zerner, M. C. (1985). A Broyden - Fletcher - Goldfarb - Shanno optimization procedure for molecular geometries. Chemical physics letters, 122(3), 264-270.

[18] Yoshida, K., Hashimoto, T., Inagaki, Y., Tagawa, H., & Dokiya, M. (1999). Crystal Structure Analysis of LaCrO3 System II. Phase Transition and Thermal Expansion of Cation-Substituted LaCrO3. ECS Proceedings Volumes, 1999(1), 657.

[19] Petousis, I., Mrdjenovich, D., Ballouz, E., Liu, M., Winston, D., Chen, W., ... & Prinz, F. B. (2017). High-throughput screening of inorganic compounds for the discovery of novel dielectric and optical materials. Scientific data, 4(1), 1-12.

[20] Padilla, J., & Vanderbilt, D. (1998). Ab initio study of SrTiO3 surfaces. Surface Science, 418(1), 64-70.

[21] Tolba, S. A., Gameel, K. M., Ali, B. A., Almossalami, H. A., & Allam, N. K. (2018). The DFT+ U: Approaches, accuracy, and applications. Density Functional Calculations-Recent Progresses of Theory and Application, 1, 5772.

[22] Himmetoglu, B., Floris, A., De Gironcoli, S., & Cococcioni, M. (2014). Hubbard-corrected DFT energy functionals: The LDA+ U description of correlated systems. International Journal of Quantum Chemistry, 114(1), 14-49.

[23] Cococcioni, M. (2012). The LDA+ U approach: a simple Hubbard correction for correlated ground states. Correlated Electrons: From Models to Materials Modeling and Simulation, 2.

[24] Song, Q. G., Song, L. L., Zhao, H., Wei, T., & Kang, J. H. (2013). The structural stabilities and electronic properties of orthorhombic and rhombohedral LaCrO3—a first-principles study. In Advanced Materials Research (Vol. 622, pp. 734-738). Trans Tech Publications Ltd.

[25] Dabaghmanesh, S., Sarmadian, N., Neyts, E. C., & Partoens, B. (2017). A first principles study of p-type defects in LaCrO 3. Physical Chemistry Chemical Physics, 19(34), 22870-22876.

[26] Li, Y. R., Hou, Z. T., Wang, T. X., Li, Y., Liu, H. Y., Dai, X. F., & Liu, G. D. (2017, May). The structural properties of LaRO3 (R= Cr, Mn, Fe): a first-principles calculation. In Journal of Physics: Conference Series (Vol. 827, No. 1, p. 012015). IOP Publishing.

[27] Adachi, H., Yakabe, H., & Yasuda, I. (2002). Hiroki Moriwake', Isao Tanaka', Kazuyoshi Tatsumi!, Yukinori Koyama'. Materials Transactions, JIM., 43(7-9), 1456.